J Therm Anal Calorim (2013) 113:379–383
DOI 10.1007/s10973-013-3251-8

Effect of milling time on thermal treatment of TiC, TiB_2/steel powders

A. Biedunkiewicz · W. Biedunkiewicz · P. Figiel · U. Gabriel-Polrolniczak · D. Grzesiak · M. Krawczyk

Received: 15 November 2012 / Accepted: 10 May 2013 / Published online: 7 June 2013

Abstract The results of investigation on influence of the milling process on mixed powders of nanocrystalline TiC and TiB_2, obtained in non-hydrolytical sol–gel synthesis, and 316L stainless steel are presented. The powders have been used as substrates to prepare nanocomposite materials by Selective Laser Sintering/Melting process. In present work thermal analysis results along with the composition and structure of nanocrystalline powders have been presented. During investigation the following analytical techniques have been applied: XRD, TEM, TG-DSC-MS and SEM.

Keywords Thermal analysis · Milling · TiC · TiB_2 · Steel composite

Introduction

It is well established that the incorporation of hard, second-phase particles suitably added to ferrous matrices can significantly improve certain material properties. Powder metallurgy roots are employed on an industrial scale to produce iron-based TiC metal matrix composites. Particulate-reinforced ferrous-based metal matrix composites exhibit both excellent wear resistance and cutting properties, and are competitive with existing materials used in heavy wear applications.

In this class of engineering materials, iron-based composites containing TiC have received particular attention [1–3]. They exhibit the toughness and machinability comparable to conventional alloy steels combined with significant improvements in hardness and wear resistance. The addition of titanium diboride (TiB_2) to metal matrices has also been observed to greatly increase stiffness, hardness and wear resistance. The TiB_2–TiC/Fe composites possess excellent wear resistance under the condition of dry sliding with heavy loads [4–6]. TiC and TiB_2 particles are expected to be the best reinforcements for steel matrix composites because of their high thermal stability at higher temperature, high modulus of elasticity, good wettability, low density and their relative stability with steel matrix [7].

Small TiC and TiB_2 particles uniformly distributed in a steel matrix are the source of strengthening of the composites. Adequate and coherent bonding between matrix and particles is essential to permit incorporation of the carbides to the maximum strength [2].

Ball milling (BM) is a solid-state powder process involving phenomena of the bonding and strengthening of the composites enhancing their properties after sintering process [8]. In the present study, the effect of BM pretreatment of the starting 316L steel, nc-TiC and nc-TiB_2 powders mixture on the non-isothermal heat treatment results is presented. This paper reports comparative results of the non-isothermal heat treatment of nc-TiC/316L steel and the nc-TiC–nc-TiB_2/316L steel systems after BM of the powder particles for different times. Thermal analysis is an effective tool able to support the elaboration of the manufacturing processes of metal matrix composites (MMC) [9].

A. Biedunkiewicz · P. Figiel · M. Krawczyk (✉)
Institute of Materials Science and Engineering,
West Pomeranian University of Technology, Szczecin,
Piastow Av. 19, Szczecin, Poland
e-mail: mkrawczyk@zut.edu.pl

W. Biedunkiewicz · D. Grzesiak
Institute of Mechanical Technology, West Pomeranian University of Technology, Piastow Av. 19, Szczecin, Poland

U. Gabriel-Polrolniczak
Department of Physics and Chemistry, Maritime University of Szczecin, Waly Chrobrego 1-2, Szczecin, Poland

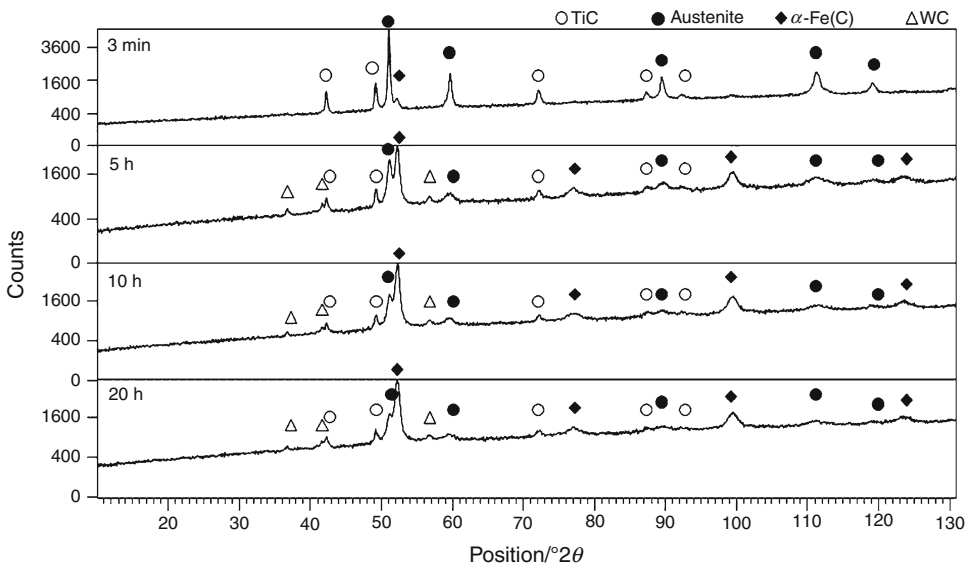

Fig. 1 Comparison of X-ray diffractograms of nc-TiC/316L steel powder system after milling for 3 min, 5, 10 and 20 h

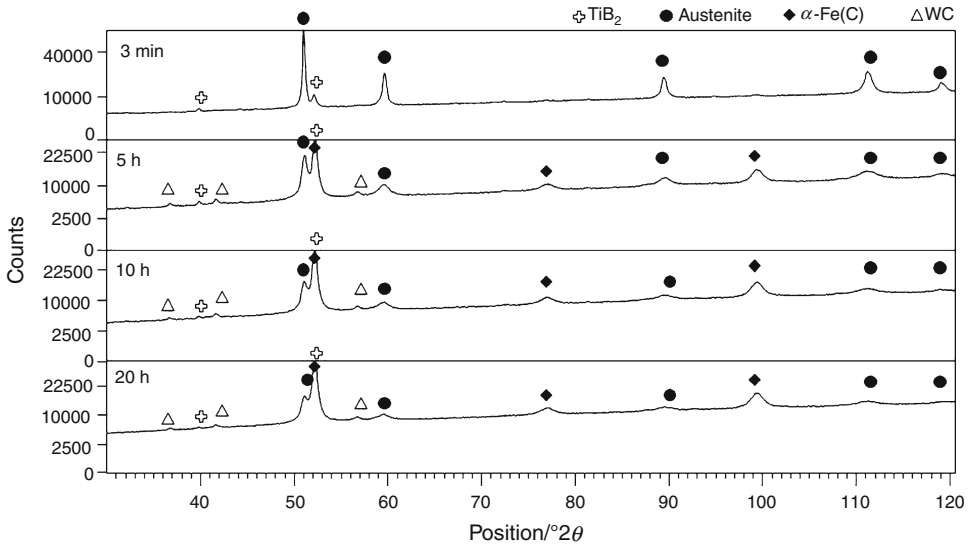

Fig. 2 Comparison of X-ray diffractograms of nc-TiC–nc-TiB_2/316L steel powder systems after milling for 3 min, 5, 10 and 20 h

Experimental

The stainless steel 1.4404 (AISI 316L) from SLM Solutions GmbH was used as matrix and, as the hard second-phase particles nc-TiC and nc-TiC–nc-TiB_2 mixture (volume ratio ca. 1:4) in powder form were used. nc-TiC and nc-TiC–nc-TiB_2 powders, containing small amounts of amorphous carbon (3–5 mass%), were obtained by non-hydrolytical sol–gel method [10]. The average size of TiC crystallites was in the range of 40–100 nm, and in case of TiC–TiB_2 equalled 60–120 nm. Microcrystalline powders of steel 316L along with the nanocrystalline powders were homogenised in planetary mill Pulverisette 4 (Fritsch GmbH), with use of the milling balls made of WC/Co in a mass ratio of 10:1 with respect to the powder, at the milling speed 300 rpm.

The samples of powder of composition 20 vol% of TiC (or TiC–TiB_2) + 80 vol% of steel 316L were milled with ethanol (30 cm^3) in a vessel of 80 cm^3 volume with 30 balls for 3 min. Then the samples were milled for 5, 10 and 20 h (7, 14 and 21 cycles, respectively). Each cycle included 45 min milling and 15 min of cooling.

The powders after 3 min, 5, 10 and 20 h of milling were successively subjected to the heating process in argon atmosphere. Thermogravimetric measurements were carried out on TG–DSC Q600 (TA Instruments) apparatus under non-isothermal conditions under atmospheric pressure. Argon of class 6.0 ($H_2O \leq 0.5$, $O_2 \leq 0.5$, $N_2 \leq 0.5$, $CnHm \leq 0.1$, $CO \leq 0.1$, $CO_2 \leq 0.1$ vpm) from Messer was used during the experiments. Argon purge flow rate during measurements was set at 100 cm^3 min^{-1}. Gaseous products of proceeding transitions were identified by mass

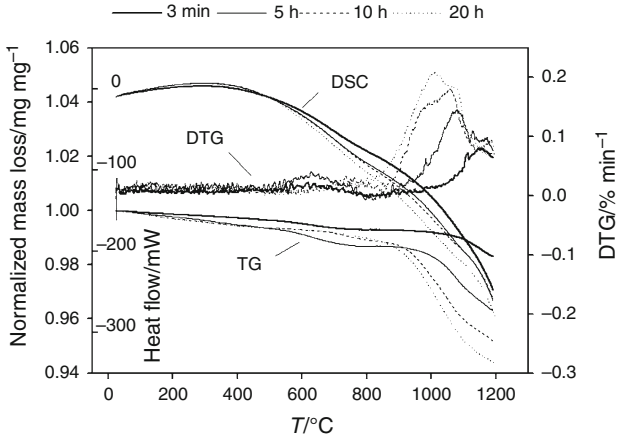

Fig. 3 Normalized mass loss, DTG and DSC dependencies on temperature obtained at sample heating rate of 10° min^{-1} during the heating up to 1,200 °C. Heating of nc-TiC/316L steel powder system after milling for 3 min, 5, 10 and 20 h in argon atmosphere

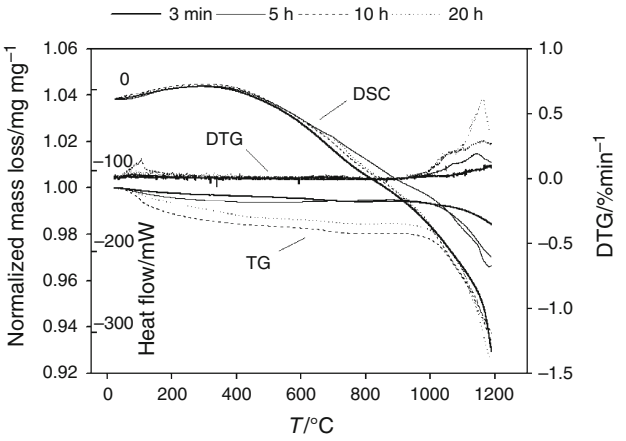

Fig. 5 Normalized mass loss, DTG, and DSC dependencies on temperature obtained for sample heating rate of 10° min^{-1} during the heating up to 1,200 °C. Heating of nc-TiC–TiB_2/316L steel powder system after milling for 3 min, 5, 10 and 20 h in argon atmosphere

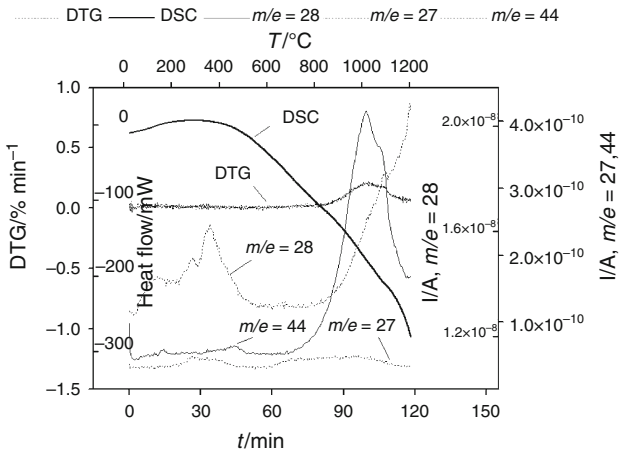

Fig. 4 Functions of DTG, DSC and mass spectra of HCN, CO and CO_2 in temperature. Heating of nc-TiC/316L steel powder system after milling for 20 h in argon, heating rate 10° min^{-1}

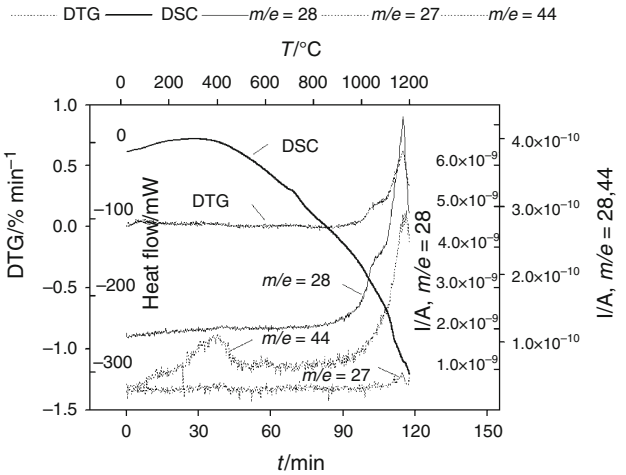

Fig. 6 Plot of DTG and DSC functions and mass spectra for m/e = 27 (BO), m/e = 28 (CO) and m/e = 44 (CO_2) of the sample of composition 20 vol% of nc-TiC–TiB_2 80 vol% of steel 316L, after milling for 20 h. Heating in argon, 10° min^{-1} up to 1,200 °C

spectrometry method. Pfeifer Vacuum ThermoStar GDS 301 apparatus was used. In all series the temperature of samples changed linearly in time. Solid products were identified by XRD method. X'Pert Pro apparatus from PANalytical with a copper X-ray tube with current voltage 35 kV and intensity 40 mA was used. Spectra processing and analysis was performed using X'Pert High Score 1.0 software with incorporated ICDD spectra library.

Results

Temperature, TG, DTG, HF functions and mass spectra of volatile products have been registered in time. The measurements were carried out in the temperature range 25–1,200 °C and at sample heating rates of 10° min^{-1} for TiC/316L and TiC–TiB_2/316L systems. Mass of the samples was in the order of 30 mg. In Fig. 1 the comparison of X-ray diffraction patterns of the nc-TiC/316L steel powder system is presented.

Analysis of phase composition of the mixture of nc-TiC and 316L steel powders after milling showed, besides the nc-TiC and austenite of steel 316L introduced into the mixture, increasing fraction of α-Fe(C) phase and contamination with material of the mill i.e. tungsten carbide WC. Comparisons of the X-ray diffraction patterns of the nc-TiC–nc-TiB_2/316L powders systems are presented in Fig. 2.

For the system of nc-TiC–nc-TiB_2/316L steel powders after milling process the same results of XRD analysis

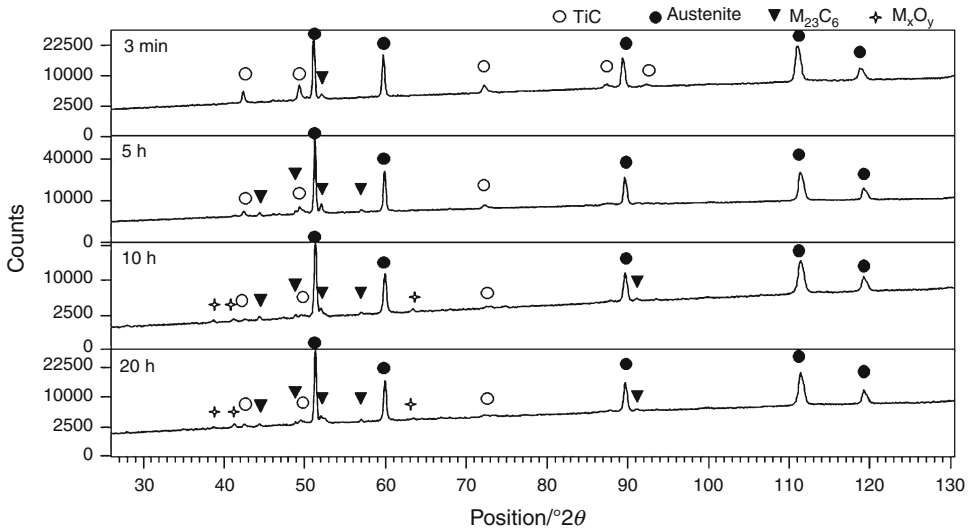

Fig. 7 XRD diffractograms of the samples of the composition 20 vol% of TiC + 80 vol% of steel 316L, after milling for 3 min, 5, 10, 20 h and heating in argon at 10° min^{-1} up to 1,200 °C

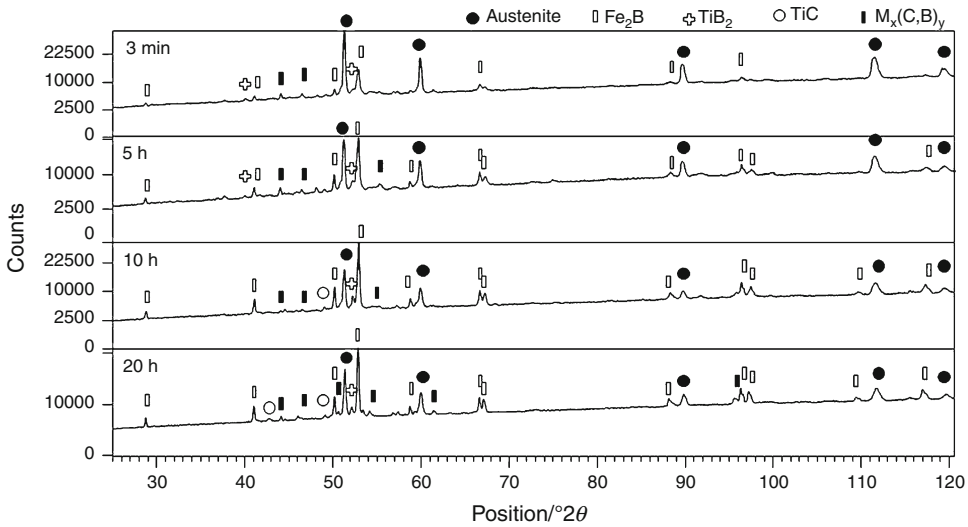

Fig. 8 XRD diffractograms of the samples of composition 20 vol% of TiC–TiB_2 80 vol% of steel 316L, after milling for 3 min, 5, 10, 20 h and heating in argon at 10° min^{-1} up to 1,200 °C

were stated. Increasing fraction of α-Fe(C) phase and contamination with material of the mill i.e. tungsten carbide WC were observed. In Fig. 3 TG, DTG and DSC dependencies on temperature obtained for nc-TiC/316L steel sample at heating rate of 10° min^{-1} were depicted. In Fig. 4 DTG, DSC functions and mass spectra of HCN, CO and CO_2 in temperature obtained for the sample after milling for 20 h were combined. While for nc-TiC–TiB_2/316L steel powder TG, DTG, DSC curves along with mass spectra of BO, CO and CO_2 are presented in Figs. 5 and 6, respectively.

Process of consolidation of the nc-TiC particles with the 316L steel powder started above temperature of 900 °C, and for nc-TiC–nc-TiB_2/316L steel system above 930 °C. In those processes two stages have been distinguished. Neither of the stages has been finished. During these stages carbon monoxide and carbon dioxide were formed at the lower and higher temperature, respectively. The longer time of milling favoured the reaction of CO_2 formation. Above results are in agreement with observations made during the investigations of initially milled nc-TiC and 316L steel powders sintering by selective laser sintering/melting (SLS/M) technique [11]. This allows formulating the hypothesis that the carbon oxides were formed as a result of reaction of elementary carbon with oxide $(Cr,Fe)_2O_3$ coating the steel 316L powders, according to endothermic reaction (1) and/or (2):

$$23Cr_2O_3 + 81C \rightarrow 2Cr_{23}C_6 + 69CO \quad (1)$$

$$46Cr_2O_3 + 93C \rightarrow 4Cr_{23}C_6 + 69CO_2 \quad (2)$$

The results of analysis of phase composition of the system nc-TiC/316L steel, after milling and heating up to temperature of 1,470 K at sample heating rate of 10 K min^{-1}, based on XRD method (Figs. 7, 8) are listed in Table 1.

Table 1 Phase composition of nc-TiC/316L steel samples after milling and heating

Milling time	Phase composition
3 min	Austenite (316L steel) + nc-TiC and probably carbide of $M_{23}C_6$ (M: Cr, Fe) type
5 h	Austenite (316L steel) + nc-TiC, and probably carbide of $M_{23}C_6$ (M: Cr, Fe) type
10 h	Austenite (316L steel) + nc-TiC, and probably carbide of $M_{23}C_6$ (M: Cr, Fe) type I and M_xO_y
20 h	Austenite (316L steel) + nc-TiC, and probably carbide of $M_{23}C_6$ (M: Cr, Fe) type I and M_xO_y

Table 2 Phase composition of nc-TiC–nc-TiB_2/316L steel samples after milling and heating

Milling time	Phase composition
3 min	Austenite (316L steel) + Fe_2B, nc-TiB_2 and probably carbide of $M_x(C,B)_y$ (M: Cr, Fe) type and TiC
5 h	Austenite (316L steel) + Fe_2B, nc-TiB_2 and probably carbide of $M_x(C,B)_y$ (M: Cr, Fe) type and TiC
10 h	Austenite (316L steel) + Fe_2B, nc-TiB_2 and probably carbide of $M_x(C,B)_y$ (M: Cr, Fe) type and TiC
20 h	Austenite (316L steel) + Fe_2B, nc-TiB_2 and probably carbide of $M_x(C,B)_y$ (M: Cr, Fe) type and TiC

The results of analysis showed that along with the increase of the milling time the fraction of carbide of $M_{23}C_6$ (M: Cr, Fe) type and M_xO_y increased.

The results of analysis of phase composition of the system nc-TiC–nc-TiB_2/316L steel, after milling and heating up to the temperature of 1,200 °C at sample heating rate of 10° min^{-1}, based on XRD method are listed in Table 2.

It was concluded that along with the increase of the milling time the fraction of carboboride of $M_{23}(C,B)_6$ (M: Cr, Fe) type, and also iron boride Fe_2B and titanium carbide TiC increased. This phenomena could be explained by the possibility of proceeding reaction $TiB_2 + 4\text{-}Fe + C{=}2Fe_2B + TiC$, for which reaction enthalpy ΔG changes from −25.5 to −17 kcal mol^{-1} in temperature range 25–1,200 °C [12].

Conclusions

Comparative results of the non-isothermal thermal treatment of the 316L steel–nc-TiC and the 316L steel—nc-TiC–nc-TiB_2 systems after BM of the powder particles for the different times have been investigated.

It was stated that along with the increase of the milling time the processes of consolidation of powders 316L steel—nc-TiC and the 316L steel—nc-TiC–nc-TiB_2 proceeded more effectively due to reaction of chromium and/or iron carbides formation with generation of carbon oxides.

The results of investigation showed that along with the increase of the time of the milling of nc-TiC–nc-TiB_2/316L steel powders the fraction of iron boride Fe_2B increased. The formation of Fe_2B was explained by the possibility of proceeding reaction of nc-TiB_2 with the steel matrix.

Acknowledgments The research was funded by The National Centre for Research and Development in the frame of the realisation of the development Project No. 15-0067-10/2010-2013 and the Dean's Grant "Young Staff" No. 517-06-010-3368/17.

References

1. Kattamis TZ, Suganuama T. Solidification processing and tribological behavior of particulate TiC-ferrous matrix composites. Mater Sci Eng A. 1990;128:241–52.
2. Parashivamurthy K, Kumar RK, Seethramu S, Chandrasekharaiah MN. Review on TiC reinforced steel composites. J Mater Sci. 2001;36:4519–30.
3. Ning L, Chengliang H, Haidong Y, Yudong X, Min S, Sheng Ch, Feng X. The milling performances of TiC-based cermet tools with TiN nanopowders addition against normalized medium carbon steel AISI1045. Wear. 2005;258:1688–95.
4. Jiang QC, Ma BX, Wang HY, Wang Y, Dong YP. Fabrication of steel matrix composites locally reinforced with in situ TiB_2–TiC particulates using self-propagating high-temperature synthesis reaction of Al–Ti–B_4C system during casting. Compos A. 2006;37:133–8.
5. Binghong L, Ying L, Jun L, Hui C, Lin H. Effect of sintering process on the microstructures and properties of in situ TiB_2–TiC reinforced steel matrix composites produced by spark plasma sintering. J Mater Proc Technol. 2010;210(1):91–5.
6. Degnan CC, Shipway PH. A comparison of the reciprocating sliding wear behaviour of steel based metal matrix composites processed from self-propagating high-temperature synthesis of Fe–TiC and Fe–TiB_2 master alloys. Wear. 2002;252:832–41.
7. Akhtar F, Shiju G, Fenge C, Peizhong F, Tao L. TiB_2 and TiC stainless steel matrix composites. Mater Lett. 2007;61(1):189–91.
8. Locci AM, Orru R, Cao G, Munir ZA. Effect of ball milling on simultaneous spark plasma synthesis and densification of TiC–TiB_2 composites. Mater Sci Eng A. 2006;434:23–9.
9. Montanaro L, Palmero P, Lombardi M, Esnouf C, Chevalier J, Cardinal S. Thermal analyses applied to ceramic nanopowders: from synthesis to sintering. A review on transition alumina powder-based materials. J Therm Anal Calorim. 2013;112:437–45.
10. Biedunkiewicz A, Gabriel U, Figiel P, Grzesiak D. Application of thermal analysis in nanotechnology. Carbonization and purification of nc-TiC_x in argon atmosphere. J Therm Anal Calorim. 2010;101(2):701–6.
11. Figiel P, Biedunkiewicz W, Grzesiak D. Oxidation process of the steel/nc-TiC nanocomposites, J Therm Anal Calorim. 2012;108:979–83.
12. Outokumpu HSC Chemistry for Windows (2002); Chemical reaction and equilibrium Software with extesive thermochemical database, version 5.1, ISBN 952-9507-08-09.